

Visualizing myosin–actin interaction with a genetically-encoded fluorescent strain sensor

Sosuke Iwai^{a,1} and Taro Q. P. Uyeda^{a,b,1}

^aResearch Institute for Cell Engineering, National Institute of Advanced Industrial Science and Technology, 1-1-1 Higashi, Tsukuba, Ibaraki 305-8562, Japan; and ^bBiomedical Information Research Center, National Institute of Advanced Industrial Science and Technology, 2-42 Aomi, Koto, Tokyo 135-0064, Japan

Edited by Peter N. Devreotes, The Johns Hopkins University School of Medicine, Baltimore, MD, and approved September 23, 2008 (received for review June 6, 2008)

Many proteins have been shown to undergo conformational changes in response to externally applied force *in vitro*, but whether the force-induced protein conformational changes occur *in vivo* remains unclear. To reveal the force-induced conformational changes, or strains, within proteins in living cells, we have developed a genetically encoded fluorescent “strain sensor,” by combining the proximity imaging (PRIM) technique, which uses spectral changes of 2 GFP molecules that are in direct contact, and myosin–actin as a model system. The developed PRIM-based strain sensor module (PriSSM) consists of the tandem fusion of a normal and circularly permuted GFP. To apply strain to PriSSM, it was inserted between 2 motor domains of *Dictyostelium* myosin II. In the absence of strain, the 2 GFP moieties in PriSSM are in contact, whereas when the motor domains are bound to F-actin, PriSSM has a strained conformation, leading to the loss of contact and a concomitant spectral change. Using the sensor system, we found that the position of the lever arm in the rigor state was affected by mutations within the motor domain. Moreover, the sensor was used to visualize the interaction between myosin II and F-actin in *Dictyostelium* cells. In normal cells, myosin was largely detached from F-actin, whereas ATP depletion or hyperosmotic stress increased the fraction of myosin bound to F-actin. The PRIM-based strain sensor may provide a general approach for studying force-induced protein conformational changes in cells.

conformational change | force | GFP | proximity imaging

Many proteins have been shown to undergo conformational changes in response to externally applied force *in vitro* (1). They include structural proteins, such as muscle and cytoskeletal proteins, which are responsible for maintaining the structural integrity of cells (2–5). On the other hand, mechanosensory proteins, which include cell adhesion proteins and proteins linked to mechanosensitive ion channels, are involved in the transduction of mechanical signals to cells (6–8). In either case, protein conformational changes are believed to play important roles in the processes, although whether they occur *in vivo* remains unclear. Recently, evidence has accumulated for force-induced protein conformational changes in cells. For instance, the Src family kinase substrate is mechanically extended in spread cells, as revealed by conformation-sensitive antibody (9). More recently, a shotgun cysteine labeling approach revealed that several cytoskeletal proteins change their conformation or assembly in mechanically stressed cells (10). Despite these studies, little is known about the spatial and temporal dynamics of the protein conformational changes in cells. To reveal the force-induced conformational changes, or strains, within proteins in living cells, a polypeptide-based fluorescent “strain sensor” would be necessary.

Fluorescent resonance energy transfer (FRET) is a technique that can measure the proximity or distance between a donor and an acceptor molecule. FRET has been widely used to detect protein conformational changes, in particular, when combined with various fluorescent proteins (11). However, FRET has a limitation in resolving protein conformational changes in cells.

FRET efficiency is usually estimated from the fluorescent intensity of samples (12), but it is known that proteins often exist in multiple conformational states (13), and the intensity-based FRET method cannot distinguish between a conformational intermediate state and a mixture of multiple states. Fluorescence lifetime microscopy combined with multicomponent analysis (14) or single-molecule imaging (13) may overcome this problem, but demand complicated apparatus and analysis. A decade ago, De Angelis *et al.* (15) reported another GFP-based technique, which they termed proximity imaging (PRIM). PRIM depends on direct contact between 2 GFP molecules, which can lead to structural perturbations and concomitant spectral changes (15, 16). Unlike FRET, PRIM is assumed to involve only 2 types of fluorescent excitation spectra corresponding to monomeric and dimeric GFP, so that an estimated excitation ratio will simply reflect a mixing ratio of the monomer and the dimer, in principle. Therefore, PRIM would be useful for detecting the protein conformational changes *in vitro* and *in vivo*.

Myosin is an actin-based motor protein that undergoes cyclical interaction with F-actin during the ATP-hydrolysis cycle. In a widely accepted model, the driving force for motion is generated as a result of conformational changes in the motor domain while attaching to F-actin (17). Such conformational changes cause distortion of an elastic element within the myosin molecule and allow strain to develop (18), which can lead to relative displacement of myosin and F-actin. Thus, the myosin and actin system is a molecular strain generator and can be used to apply strain to the polypeptide-based sensor in solution. In this study, we have used *Dictyostelium* myosin II and actin as a model system to characterize the strain sensor. By combining the GFP-based PRIM technique and myosin–actin as the model system, we developed a genetically encoded fluorescent sensor that can detect force-induced conformational changes, or strains, within proteins. Using the sensor system, we found that the position of the lever arm in the rigor state was affected by mutations within the motor domain. Moreover, the sensor was used to visualize the interaction between myosin II and F-actin in *Dictyostelium* cells.

Results

Optimization of GFP Concatemer for PRIM. We first sought to optimize GFP concatemer for the PRIM technique. In the first report on PRIM (15), 2 natural GFP molecules were joined in tandem to provide a test case for PRIM, but the spectral changes caused by the covalent linking were relatively small. The crystal

Author contributions: S.I. and T.Q.P.U. designed research; S.I. performed research; S.I. analyzed data; and S.I. and T.Q.P.U. wrote the paper.

The authors declare no conflict of interest.

This article is a PNAS Direct Submission.

¹To whom correspondence may be addressed. E-mail: iwai-sosuke@aist.go.jp or t-uyeda@aist.go.jp.

This article contains supporting information online at www.pnas.org/cgi/content/full/0805513105/DCSupplemental.

© 2008 by The National Academy of Sciences of the USA

a fluorescence property similar to that of monomeric GFP. Upon addition of ATP, the motor domains would detach from F-actin, which can lead to the relief of the strain and a concomitant reversal of the spectral change.

PriSSM-motor was expressed in *Dictyostelium* cells and purified by ATP extraction of a Triton-insoluble cytoskeleton fraction and nickel affinity chromatography using the His tag fused to the C terminus of the protein. The purified protein changed the fluorescence excitation spectra in actin and/or ATP-dependent manners (Fig. 2C). As expected, $R_{490/390}$ increased >2-fold upon addition of F-actin (Fig. 2D, PriSSM-motor). The $R_{490/390}$ in the absence and presence of actin were comparable to that of the GFP concatemer and monomer, respectively. This finding suggested that, when both of the motor domains formed rigor complexes with F-actin, the protein was in a strained conformation and the 2 GFP moieties lost their contact. This process was ATP-independent, suggesting that the intramolecular association between the 2 GFP moieties was disrupted by thermal activation without the help of active force developed by the myosin motor. $R_{490/390}$ decreased when ATP was added and then increased again when apyrase was added, suggesting that the conformational and spectral changes of PriSSM-motor were reversible. In the presence of both ADP and actin, PriSSM-motor showed an $R_{490/390}$ similar to that in the rigor state, consistent with the model that the myosin motor domain attached to F-actin does not undergo a major conformational change accompanying ADP release (17). Collectively, the PriSSM-motor showed high and low values for $R_{490/390}$ (dynamic range, >100%), corresponding to the strained and unstrained states, respectively, confirming that PriSSM functions as a strain sensor module.

When PriSSM-motor is bound to F-actin in the absence of ATP, the lever arm of the N-terminal motor domain would be in the poststroke position with regard to F-actin, which may produce the strained state of the sensor. To confirm this idea, 3 residues at the base of the lever arm within the N-terminal motor domain (Ile-766, Lys-767, Ala-768) were replaced with glycine residues (Fig. 2A, PriSSM-GGG). The change in $R_{490/390}$ for PriSSM-GGG on addition of F-actin was significantly smaller than that for PriSSM-motor (Fig. 2D), supporting the idea that the lever arm is in the poststroke orientation to F-actin when the sensor is in the strained state, and also suggesting that the rigidity of the lever arm is important for its orientation. Strong binding of the motor domain to F-actin is also thought to be important for the lever arm conformation (17). To examine whether the lever arm position in PriSSM-motor depends on the strong binding, the cardiomyopathy loop within the N-terminal motor domain, which is involved in the strong binding (26), was deleted (Fig. 2A, PriSSM- Δ CMN). The deletion caused a smaller change in $R_{490/390}$ (Fig. 2D), suggesting that the strong binding to F-actin is important for maintaining the position of the lever arm relative to F-actin. Likewise, the deletion of the loop within the C-terminal motor domain (Fig. 2A, PriSSM- Δ CMC) also caused a smaller change in $R_{490/390}$ (Fig. 2D). The results of the cardiomyopathy loop deletions together suggest that, when the sensor is in the strained state with a high $R_{490/390}$, both of the motor domains are mostly in the strongly bound state.

Visualization of Myosin-Actin Interaction in Cells. PriSSM-motor showed the ratiometric and reversible spectral changes when attached to F-actin, allowing us to detect the interaction of myosin with F-actin in cells by using the sensor. To detect the behavior of intact myosin II, the C-terminal His tag of PriSSM-motor was eliminated and replaced with the myosin tail domain to produce PriSSM-myosin (Fig. 3A). To examine whether PriSSM-myosin retains physiological functions, the protein was expressed in myosin II-null cells. *Dictyostelium* myosin II-null cells are unable to divide in suspension culture or form fruiting

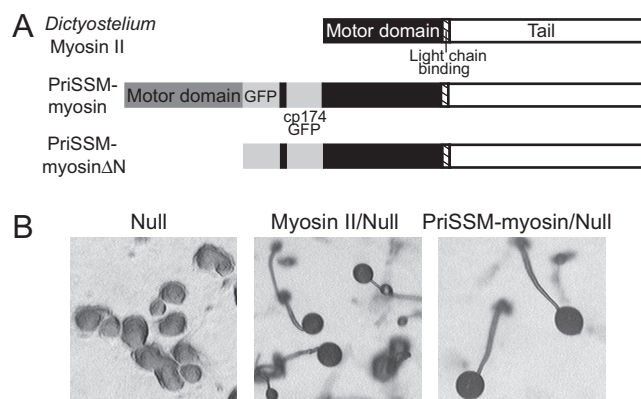


Fig. 3. Expression of myosin II-PriSSM fusion proteins in *Dictyostelium* cells. (A) Domain structures of *Dictyostelium* myosin II and its PriSSM-fusion proteins. (B) Development of fruiting bodies. Myosin-null cells (Left), myosin-null cells expressing wild-type myosin II (Center), and PriSSM-myosin (Right) were seeded onto bacterial lawns and allowed to develop for 7 days at 22°C.

bodies when starved, providing evidence that myosin II is involved in cytokinesis and morphogenesis (27, 28). Myosin II-null cells expressing PriSSM-myosin divided normally in suspension culture (data not shown) and developed completely to form normal fruiting bodies comparable to those formed by the cells expressing wild-type myosin II (Fig. 3B). These results suggest that PriSSM-myosin retains physiological functions for myosin II and is expected to behave like native myosin II in cells. For imaging studies, PriSSM-myosin was expressed in wild-type *Dictyostelium* cells to form a heterodimer with endogenous myosin II, to reduce nonspecific GFP-GFP interactions, which might occur in homodimeric PriSSM-myosin.

The cells expressing PriSSM-myosin were suspended in buffer and measured for fluorescence excitation spectra (Fig. 4A Upper Left). Because the measured spectrum contained a considerable amount of autofluorescence of cells, the autofluorescence was measured independently by using control *Dictyostelium* cells, and the contributions from PriSSM-myosin and the autofluorescence were separated by means of a linear unmixing procedure (29). The contribution from PriSSM-myosin was composed mostly of the spectrum of the purified PriSSM-motor in the presence of ATP with the low $R_{490/390}$ value. This finding suggests that at least 1 of the 2 motor domains of PriSSM-myosin is mostly detached from F-actin in cells, because the sensor would show a high $R_{490/390}$ value if both of the motor domains are bound. When *Dictyostelium* cells are treated with sodium azide, which depletes cellular ATP, they round up and contract (30). Fluorescence excitation spectrum of PriSSM-myosin in azide-treated cells was also measured (Fig. 4A Upper Right). In contrast to the cells in normal buffer, azide-treated cells showed relatively high $R_{490/390}$ values (Fig. 4A Lower Right), suggesting that the ATP depletion increased the fraction of PriSSM-myosin that was bound to F-actin. Similarly, addition of 350 mM sorbitol significantly increased $R_{490/390}$ (Fig. 4A Lower Right), suggesting that hyperosmotic stress also increased the fraction of PriSSM-myosin bound to F-actin. Although these external stimuli reduced the fluorescence intensity of the sensor probably by acidifying the cytosol (31), $R_{490/390}$ of PriSSM was not affected by pH changes between pH 6 and 8 [supporting information (SI) Fig. S1].

Triton-insoluble cytoskeletons, or Triton ghosts, contain actin and myosin II as major components (32, 33) and are suitable for initial microscopic observations of PriSSM-myosin. The cells expressing PriSSM-myosin were attached onto a glass surface and lysed with 0.5% Triton X-100 to obtain Triton ghosts containing PriSSM-myosin. Fluorescent images of the Triton ghosts were acquired under excitation at 380 ± 15 or 480 ± 15

single motor domain would be at most <10%. This idea is consistent with the notion that the nonmuscle myosin II proteins are largely detached from F-actin in cells, which is explained by the 2 previously reported properties of the protein. First, most of the *Dictyostelium* myosin II proteins normally exist as a monomer in the cytoplasmic pool (38), which is separated from F-actin-enriched cellular structures. Second, under the cellular concentration of ATP, myosin II is a typical motor with a low duty ratio and is mostly detached from F-actin, even when assembled into thick filaments (39). In contrast to the normal cells, cells treated with azide or DNP, which deplete cellular ATP, showed an increase in the fraction of the motor domain that was bound to F-actin. This outcome suggests that the contraction of cells by ATP depletion results from the increased binding of myosin II. Under hyperosmotic conditions, *Dictyostelium* cells are known to rearrange their cytoskeletal proteins including myosin II and actin (40, 41). We found that hyperosmotic stress also increased the fraction of the motor domain bound to F-actin, which may be at least partly caused by the decrease in the cellular nucleoside triphosphate level under hypertonic conditions (31). The increased binding of myosin II may contribute to maintaining cortical tension to protect cells against the osmotic stress.

When the 2 motor domains of PriSSM-motor were bound to F-actin, the intramolecular association between the 2 GFP moieties was disrupted by thermal activation without the help of active force developed by the myosin motor. The separated state was maintained stably in the presence of F-actin and in the absence of ATP, suggesting that the bond strength between the GFP moieties is smaller than that between myosin and F-actin, of which unbinding force is several piconewtons under a slowly applied load (42). In addition, several groups (22, 43) reported the dissociation constant of dimeric GFP to be $\approx 100 \mu\text{M}$. In the model for a thermally activated dissociation under an applied load, the pulling force lowers the activation energy barrier governing the dissociation kinetics (44). Thus, unbinding forces are assumed to correlate with spontaneous dissociation rates and consequently dissociation constants in solution, as shown for antibody-antigen complexes (45). If this is so for the GFP-GFP and other protein-protein interactions, it is relevant that the GFP-GFP interaction has a smaller unbinding force than other physiological protein-protein interactions, of which dissociation constants are usually in the micromolar range or less. The smaller bond strength between the GFP moieties implies an extremely high "sensitivity" of the current strain sensor. However, a detailed structure of the dimeric GFP would offer clues for modifying the dimer interface to enhance the dimer association (19, 43). These modifications may increase the unbinding force of the GFP moieties and thereby allow us to tune the strain sensor. Moreover, engineering of GFP, especially in the amino acid residues close to the chromophore, has produced mutants with shifted excitation spectra (46). These mutations may also improve the spectral properties of the sensor.

To date, many proteins have been shown to undergo conformational changes in response to externally applied force in vitro (1), but whether the force-induced conformational changes occur in vivo remains largely unknown. The strain sensor module developed in this study may be incorporated into other proteins and contribute to elucidating the spatial and temporal dynamics of their force-induced conformational changes in living cells. During the course of our study, Meng *et al.* (47) reported a FRET-based mechanical stress sensor. The sensor depends on force-induced unfolding of an α -helix between 2 fluorescent proteins and seems to have a relatively high unfolding force of tens of piconewtons. Thus, our PRIM-based sensor, which is at present suitable for detecting relatively small force of several piconewtons, would complement the FRET-based sensor. Given the possibility of the tuning, the PRIM-based strain sensor,

together with other sensors, may provide a general approach for studying force-induced protein conformational changes in cells.

Materials and Methods

Expression and Purification of Proteins. For expression of GFP concatemers, cDNAs encoding GFP or the cpGFP both carrying the F64L/S65T mutations (46) were amplified by PCR and ligated into pET-30b(+) (Novagen) with linker sequences containing GGS repeats. cDNA encoding cpGFP with the N terminus at Gly-174 was amplified according to ref. 48. All GFP-derived proteins were expressed in *Escherichia coli* Rosetta(DE3) (Novagen) at 22° C for 7 h. The proteins were purified by using an Ni-nitrilotriacetic agarose (Qiagen) column and dialyzed against an assay buffer [10 mM Hepes (pH 7.4), 50 mM KCl, 2 mM MgCl₂, and 1 mM DTT]. In some cases, the proteins were further incubated overnight at room temperature to facilitate protein folding and chromophore formation. Concentrations of the GFP-derived proteins were determined by the Bradford method using GFP as a standard.

For expression of PriSSM-motor and PriSSM-myosin, cDNAs encoding a *Dictyostelium* myosin II heavy chain fragment (residues 1–768), the GFP concatemer with a 29-aa linker, and the other myosin heavy chain fragment (residues 3–761 or 3–2116) were ligated into pTIKL extrachromosomal expression vector (49). A polyhistidine tag was placed at the C terminus of PriSSM-motor. For PriSSM-GGG, PriSSM- Δ CMN, and PriSSM- Δ CMC mutants, the mutations were introduced into PriSSM-motor by PCR-based methods. The expression vectors were introduced into *Dictyostelium* Ax2 wild-type cells or HS1 cells lacking the endogenous myosin II heavy chain gene (27) by electroporation. All transformants were selected in HL5 medium containing 10 $\mu\text{g}/\text{mL}$ G418.

For purification of PriSSM-motor and its mutants, Ax2 cells expressing the proteins were washed and resuspended in 2 vol/g of a lysis buffer [10 mM Hepes (pH 7.4), 10 mM KCl, 5 mM EGTA, and 2 mM MgCl₂] containing 1 mM DTT and protease inhibitors, and lysed by addition of Triton X-100 to a final concentration of 2%. Triton-insoluble cytoskeleton was collected by centrifugation at 20,000 $\times g$ for 5 min. Once washed with the lysis buffer, the cytoskeleton was extracted with a buffer containing 10 mM Hepes (pH 7.4), 50 mM NaCl, 1 mM EGTA, 5 mM MgCl₂, 2 mM ATP, and 1 mM DTT and centrifuged at 300,000 $\times g$ for 20 min. The resultant supernatant was incubated with Ni Sepharose 6 Fast Flow (GE Healthcare) for 2 h at 4° C. The resin with the bound proteins was washed and then extracted with a buffer containing 10 mM Hepes (pH 7.4), 300 mM imidazole (pH 7.4), 500 mM NaCl, and 1 mM DTT. The extracted protein was finally dialyzed against the assay buffer and clarified by ultracentrifugation. F-actin was prepared from rabbit skeletal muscle according to Spudich and Watt (50).

Fluorescence Spectroscopy. Fluorescence excitation spectra were measured by using a fluorescence spectrophotometer (RF-5300PC; Shimadzu) at 22° C with the emission wavelength at 510 nm. Spectra of purified proteins were measured at 0.1–0.2 μM in the assay buffer. F-actin and nucleotides were added to a final concentration of 1 μM and 1 mM, respectively. To remove ATP and ADP, the reaction mixture was supplemented with 3 units/ml apyrase (Sigma) and incubated at 22° C for 10 min. To measure the spectra of cells, Ax2 cells or Ax2 cells expressing PriSSM-myosin were washed and resuspended in 20 mM Mes (pH 6.8) at a density of 3×10^6 cells/mL. The cell suspensions were gently agitated at 22° C for 30 min with or without 10 mM sodium azide before the measurements. For hyperosmotic shock, the cells were agitated for another 5 min with 350 mM sorbitol. The measured spectra of cells were separated by a non-negative least-squares method.

Fluorescence Microscopy. For observation of Triton ghosts, Ax2 cells expressing PriSSM-myosin or PriSSM-myosin Δ N were washed and suspended in an observation buffer [20 mM Mes (pH 6.8), 5 mM MgCl₂, and 0.1 mM EGTA] and allowed to settle onto a glass coverslip (22 \times 32 mm; Matsunami) for 30 min. Immediately before extraction, a flow chamber was made by placing a glass coverslip (18 \times 18 mm) over the cells with a support of double-sided adhesive tape. The cells were lysed by introducing the lysis buffer containing 0.5% Triton X-100, 1 mM DTT, 1 μM phalloidin (Sigma), and protease inhibitors, followed by incubation at 4° C for 10 min. Then the chamber was washed 3 times with the lysis buffer containing 5 mM MgCl₂ and 1% β -mercaptoethanol. For addition of ATP, the chamber was filled with the lysis buffer containing 10 mM MgCl₂, 1% β -mercaptoethanol, and 0.2 mM ATP.

For observation of living cells, Ax2 cells expressing PriSSM-myosin or PriSSM-myosin Δ N were incubated for 2–3 h in a buffer containing 10 mM Mes (pH 6.8). Then the cells were washed and suspended in the observation buffer with or without 200 μM DNP (Sigma) and allowed to settle onto a glass coverslip (22 \times 32 mm) for 10–30 min. The cells were overlaid by a thin agarose

sheet (34) and incubated for another 30 min. To make observation chambers, 2 strips of 0.2-mm-thick filter paper were placed along the sides of the agarose sheet as spacers. The agarose and the filter paper were enclosed by a layer of silicon grease and then covered with a second glass coverslip (22 × 22 mm).

The Triton ghosts or the cells were observed at 22° C by using an Olympus IX71 inverted microscope equipped with a 100× UPlanApo oil-immersion objective. For excitation, light from the mercury lamp was reduced to 25% and selected with a D380/30× or D480/30× band-pass filter (Chroma). Fluorescence images were obtained through a 500DCXR dichromatic mirror and a D535/40m band-pass filter (Chroma) and collected on a cooled charge-coupled

device camera ORCA-ER (Hamamatsu) controlled by IPLab software (Scanalytics). The images were analyzed by using a customized plugin for ImageJ (<http://rsb.info.nih.gov/ij/>).

ACKNOWLEDGMENTS. We thank Dr. Akira Nagasaki (National Institute of Advanced Science and Technology) for help with fluorescence microscopy and Dr. Eisaku Katayama (Institute of Medical Science, University of Tokyo) for continuous encouragement. This work was supported by the SENTAN (Development of System and Technology for Advanced Measurement and Analysis) program of the Japan Science and Technology Agency.

- Forman JR, Clarke J (2007) Mechanical unfolding of proteins: Insights into biology, structure, and folding. *Curr Opin Struct Biol* 17:58–66.
- Tskhovrebova L, Trinick J, Sleep JA, Simmons RM (1997) Elasticity and unfolding of single molecules of the giant muscle protein titin. *Nature* 387:308–312.
- Rief M, Gautel M, Oesterhelt F, Fernandez JM, Gaub HE (1997) Reversible unfolding of individual titin immunoglobulin domains by AFM. *Science* 276:1109–1112.
- Kellermayer MS, Smith SB, Granzier HL, Bustamante C (1997) Folding–unfolding transitions in single titin molecules characterized with laser tweezers. *Science* 276:1112–1116.
- Rief M, Pascual J, Saraste M, Gaub HE (1999) Single-molecule force spectroscopy of spectrin repeats: Low unfolding forces in helix bundles. *J Mol Biol* 286:553–561.
- Forman JR, Qamar S, Paci E, Sandford RN, Clarke J (2005) The remarkable mechanical strength of polycystin-1 supports a direct role in mechanotransduction. *J Mol Biol* 349:861–871.
- Qian F, Wei W, Germino G, Oberhauser A (2005) The nanomechanics of polycystin-1 extracellular region. *J Biol Chem* 280:40723–40730.
- Lee G, et al. (2006) Nanospring behavior of ankyrin repeats. *Nature* 440:246–249.
- Sawada Y, et al. (2006) Force sensing by mechanical extension of the Src family kinase substrate p130Cas. *Cell* 127:1015–1026.
- Johnson CP, Tang HY, Carag C, Speicher DW, Discher DE (2007) Forced unfolding of proteins within cells. *Science* 317:663–666.
- Li IT, Pham E, Truong K (2006) Protein biosensors based on the principle of fluorescence resonance energy transfer for monitoring cellular dynamics. *Biotechnol Lett* 28:1971–1982.
- Jares-Erijman EA, Jovin TM (2003) FRET imaging. *Nat Biotechnol* 21:1387–1395.
- Weiss S (2000) Measuring conformational dynamics of biomolecules by single-molecule fluorescence spectroscopy. *Nat Struct Biol* 7:724–729.
- Wallrabe H, Periasamy A (2005) Imaging protein molecules using FRET and FLIM microscopy. *Curr Opin Biotechnol* 16:19–27.
- De Angelis DA, Miesenböck G, Zemelman BV, Rothman JE (1998) PRIM: Proximity imaging of green fluorescent protein-tagged polypeptides. *Proc Natl Acad Sci USA* 95:12312–12316.
- Ward WW, Prentice HJ, Roth AF, Cody CW, Reeves SC (1982) Spectral perturbations of the *Aequorea* green fluorescent protein. *Photochem Photobiol* 35:803–808.
- Geeves MA, Holms KC (1999) Structural mechanism of muscle contraction. *Annu Rev Biochem* 68:687–728.
- Huxley AF (1957) Muscle structure and theories of contraction. *Prog Biophys Biophys Chem* 7:255–318.
- Yang F, Moss LG, Phillips GN, Jr (1996) The molecular structure of green fluorescent protein. *Nat Biotechnol* 14:1246–1251.
- Baird GS, Zacharias DA, Tsien RY (1999) Circular permutation and receptor insertion within green fluorescent proteins. *Proc Natl Acad Sci USA* 96:11241–11246.
- Topell S, Hennecke J, Glockshuber R (1999) Circularly permuted variants of the green fluorescent protein. *FEBS Lett* 457:283–289.
- Zeng W, et al. (2006) Resonance energy transfer between green fluorescent protein variants: Complexities revealed with myosin fusion proteins. *Biochemistry* 45:10482–10491.
- Rayment I, et al. (1993) Three-dimensional structure of myosin subfragment-1: A molecular motor. *Science* 261:50–58.
- Uyeda TQP, Abramson PD, Spudich JA (1996) The neck region of the myosin motor domain acts as a lever arm to generate movement. *Proc Natl Acad Sci USA* 93:4459–4464.
- Chow D, Srikulam R, Chen Y, Winkelmann DA (2002) Folding of the striated muscle myosin motor domain. *J Biol Chem* 277:36799–36807.
- Sasaki N, Asukagawa H, Yasuda R, Hiratsuka T, Sutoh K (1999) Deletion of the myopathy loop of *Dictyostelium* myosin II and its impact on motor functions. *J Biol Chem* 274:37840–37844.
- De Lozanne A, Spudich JA (1987) Disruption of the *Dictyostelium* myosin heavy chain gene by homologous recombination. *Science* 236:1086–1091.
- Knecht DA, Loomis WF (1987) Antisense RNA inactivation of myosin heavy chain gene expression in *Dictyostelium discoideum*. *Science* 236:1081–1086.
- Zimmermann T, Rietdorf J, Pepperkok R (2003) Spectral imaging and its applications in live cell microscopy. *FEBS Lett* 546:87–92.
- Pasternak C, Spudich JA, Elson EL (1989) Capping of surface receptors and concomitant cortical tension are generated by conventional myosin. *Nature* 341:549–551.
- Pintsch T, Satre M, Klein G, Martin JB, Schuster SC (2001) Cytosolic acidification as a signal mediating hyperosmotic stress responses in *Dictyostelium discoideum*. *BMC Cell Biol* 2:9.
- Yumura S, Fukui Y (1985) Reversible cyclic AMP-dependent change in distribution of myosin thick filaments in *Dictyostelium*. *Nature* 314:194–196.
- Reines D, Clarke M (1985) Immunochemical analysis of the supramolecular structure of myosin in contractile cytoskeletons of *Dictyostelium amoebae*. *J Biol Chem* 260:14248–14254.
- Yumura S, Mori H, Fukui Y (1984) Localization of actin and myosin for the study of ameboid movement in *Dictyostelium* using improved immunofluorescence. *J Cell Biol* 99:894–899.
- Neujahr R, et al. (1997) Three-dimensional patterns and redistribution of myosin II and actin in mitotic *Dictyostelium* cells. *J Cell Biol* 139:1793–1804.
- Jungbluth A, et al. (1994) Strong increase in the tyrosine phosphorylation of actin upon inhibition of oxidative phosphorylation: Correlation with reversible rearrangements in the actin skeleton of *Dictyostelium* cells. *J Cell Sci* 107:117–125.
- Warshaw DM, et al. (2000) The light chain binding domain of expressed smooth muscle heavy meromyosin acts as a mechanical lever. *J Biol Chem* 275:37167–37172.
- Egelhoff TT, Brown SS, Spudich JA (1991) Spatial and temporal control of nonmuscle myosin localization: Identification of a domain that is necessary for myosin filament disassembly in vivo. *J Cell Biol* 112:677–688.
- Howard J (1997) Molecular motors: Structural adaptations to cellular functions. *Nature* 389:561–567.
- Kuwayama H, Ecke M, Gerisch G, Van Haastert PJ (1996) Protection against osmotic stress by cGMP-mediated myosin phosphorylation. *Science* 271:207–209.
- Zischka H, et al. (1999) Rearrangement of cortex proteins constitutes an osmoprotective mechanism in *Dictyostelium*. *EMBO J* 18:4241–4249.
- Nishizaka T, Miyata H, Yoshikawa H, Ishiwata S, Kinoshita K, Jr (1995) Unbinding force of a single motor molecule of muscle measured using optical tweezers. *Nature* 377:251–254.
- Phillips GN, Jr (1997) Structure and dynamics of green fluorescent protein. *Curr Opin Struct Biol* 7:821–827.
- Evans EA, Calderwood DA (2007) Forces and bond dynamics in cell adhesion. *Science* 316:1148–1153.
- Schwesinger F, et al. (2000) Unbinding forces of single antibody-antigen complexes correlate with their thermal dissociation rates. *Proc Natl Acad Sci USA* 97:9972–9977.
- Tsien RY (1998) The green fluorescent protein. *Annu Rev Biochem* 67:509–544.
- Meng F, Suchyna TM, Sachs F (2008) A fluorescence energy transfer-based mechanical stress sensor for specific proteins in situ. *FEBS J* 275:3072–3087.
- Nagai T, Yamada S, Tominaga T, Ichikawa M, Miyawaki A (2004) Expanded dynamic range of fluorescent indicators for Ca²⁺ by circularly permuted yellow fluorescent proteins. *Proc Natl Acad Sci USA* 101:10554–10559.
- Liu X, Ito K, Lee RJ, Uyeda TQ (2000) Involvement of tail domains in regulation of *Dictyostelium* myosin II. *Biochem Biophys Res Commun* 271:75–81.
- Spudich JA, Watt S (1971) The regulation of rabbit skeletal muscle contraction. *J Biol Chem* 246:4866–4871.